Theoretical Studies on the Structure, Stability, Ability To Undergo Internal Transformations, and Tautomerization, as Well as Reactivity, of H_2PPH_2 and $HPPH_3$ Molecules

Janusz Rak,* Piotr Skurski, Adam Liwo, and Jerzy Błażejowski*

Contribution from the Department of Chemistry, University of Gdańsk, 80-952 Gdańsk, Sobieskiego 18, Poland

Received August 15, 1994[⊗]

Abstract: Semiempirical MNDO, AM1, and PM3, as well as *ab initio*, studies applying the STO-3G, 4-31G, 6-31G**, DZV, and DZP basis sets and also including the MP4 and QCISD(T) corrections were carried out on two tautomeric phosphorus hydrides H_2PPH_2 and $HPPH_3$ and uni- and bimolecular reactions. First, the geometry of the two molecules was optimized using the theoretical methods mentioned in the Hartree-Fock (HF) scheme. The energies of the molecules at stationary points corresponding to HF/6-31G** geometries were subsequently calculated including electron correlation effects on the level of the fourth-order Møller-Plesset (MP4) perturbation theory or quadratic configuration interaction with single and double substitutions and triples contribution (QCISD(T)) calculated using the 6-311+G(3df,2p) or 6-311++G(3df,3pd) basis set. Complete geometry optimizations at the MP4/6-31G** level resulted in only slight changes in the geometry and energy of the molecules as compared with HF results. In order to compare *ab initio* results with the available thermochemical data, the energies of formation of all the entities were first calculated following Hess's Law. The partition function contributions were subsequently determined in a harmonic approximation, which allowed for the calculation of entropies, heat capacities, and enthalpies and free enthalpies of formation of gaseous hydrides. This also resulted in vibrational frequencies that have to be scaled by a factor of 0.889 to suit available experimental data. Other physicochemical characteristics of the hydrides, such as dipole moments and energies of the lowest unoccupied (LUMO) and highest occupied (HOMO) molecular orbitals were obtained from theoretical calculations. The results of our *ab initio* calculations indicate unambiguously that H_2PPH_2 is thermodynamically more stable than $HPPH_3$, while the AM1 and PM3 semiempirical methods predict the reverse order of thermodynamic stability. Further, theoretical calculations predict that the H_2PPH_2 molecule can exist equally well in both gauche and staggered forms. To gain insight into the stability of the hydrides, energy changes for internal transformations (rotation around the P-P bond and inversion at P in H_2PPH_2), intramolecular (unimolecular) and intermolecular (bimolecular) hydrogen transfer, and decomposition processes were determined. Combination of these data with classical thermodynamic and kinetic (RRKM theory) considerations revealed that increasing temperature should cause the decomposition of H_2PPH_2 rather than transformation to $HPPH_3$. On the other hand, an isolated $HPPH_3$ molecule once created would be stable at ambient temperature since barriers for its unimolecular tautomerization or decomposition are relatively high. However, bimolecular tautomerization, proceeding with a negligibly small kinetic barrier over the thermodynamic one, would bring the system to the lowest energy H_2PPH_2 structure.

Introduction

Diphosphine (H_2PPH_2) (**1** and **2**) reported in the early literature[1] is one of the simplest phosphorus compounds.[2,3] Some of its properties have already been determined experimentally.[1-19] On the other hand, so far, $HPPH_3$ (**3**), which can be considered to be a tautomeric form relative of H_2PPH_2, has been neither reported nor examined theoretically. We did not think the $HPPH_3$ molecule worthy of consideration until we noted that semiempirical AM1 and PM3 methods, used to examine thermal processes involving H_3CPH_2, predicted higher thermodynamic stability for $HPPH_3$ and its derivatives than for H_2PPH_2 and related compounds. This unexpected finding encouraged us to examine thoroughly what can truly be said about the geometry and stability of both above-mentioned tautomeric molecules and whether phosphorus hydrides with unusual chemical structures can exist.

The structure and properties of diphosphine have been the subject of numerous experimental[10-19] and theoretical[20-37]

[⊗] Abstract published in *Advance ACS Abstracts*, February 1, 1995.

(1) Royen, P.; Hill, K. *Z. Anorg. Allg. Chem.* **1936**, *229*, 97.
(2) Mellor, J. W. *A Comprehensive Treatise on Inorganic and Theoretical Chemistry*; Longmans: London, 1971; Vol. 8, Suppl. 3 (phosphorus).
(3) Van Wazer, J. R. *Phosphorus and Its Compounds*; Interscience Publishers, Inc.: New York, 1958; Vol. 1, p 217.
(4) Royen, P. *Z. Anorg. Allg. Chem.* **1936**, *229*, 112.
(5) Rosenbaum, O.; Neuert, H. *Z. Naturforsch.* **1954**, *9a*, 990.
(6) Evers, E. C.; Street, E. H. *J. Am. Chem. Soc.* **1956**, *78*, 5726.
(7) Gunn, S. R.; Green, L. G. *J. Phys. Chem.* **1961**, *65*, 779.
(8) Saalfeld, F. E.; Svec, H. J. *Inorg. Chem.* **1963**, *2*, 50.
(9) Fehlner, T. P. *J. Am. Chem. Soc.* **1966**, *88*, 1819, 2613.
(10) Nixon, E. R. *J. Phys. Chem.* **1956**, *60*, 1054.
(11) Braudler, M.; Schmidt, L. *Z. Anorg. Allg. Chem.* **1957**, *289*, 219.
(12) Braudler, M.; Schmidt, L. *Naturwissenschaften* **1957**, *44*, 488.
(13) Lynden-Bell, R. M. *Trans. Faraday Soc.* **1961**, *57*, 888.
(14) Frankiss, S. G. *Inorg. Chem.* **1968**, *7*, 1931.
(15) Beagley, B.; Conrad, A. R.; Freeman, J. M.; Monaghan, J. J.; Norton, B. G.; Holywell, G. C. *J. Mol. Struct.* **1972**, *11*, 371.
(16) Durig, J. R.; Carreira, L. A.; Odom, J. D. *J. Am. Chem. Soc.* **1974**, *96*, 2688.
(17) Odom, J. D.; Wurrey, C. J.; Carreira, L. A.; Durig, J. R. *Inorg. Chem.* **1975**, *14*, 2849.
(18) Elbel, S.; Dieck, H. T.; Becker, G.; Ensslin, W. *Inorg. Chem.* **1976**, *15*, 1235.
(19) Braudler, M.; Vogel-Braudschus, M.; Dobbers, J. *Z. Anorg. Allg. Chem.* **1977**, *347*, 78.
(20) Issleib, K.; Grundler, W. *Theor. Chim. Acta* **1968**, *11*, 107.

0002-7863/95/1517-2638$09.00/0

studies. Infrared,[10,17] Raman,[11,12,17,19] microwave,[16] electron diffraction,[15] photoelectron,[18] and ^{31}P-NMR[13] investigations seem to indicate that the molecule of diphosphine adopts a gauche (**1**) conformation in gaseous,[10,15,17,18] liquid,[11-13,16,19] and solid[17] phases, while X-ray,[10] as well as some infrared[10,14] and Raman,[14] studies on solid diphosphine do not rule out the possibility of the existence of the staggered (**2**) form. Moreover, the results of some investigations do not exclude the possibility of the coexistence of **1** and **2** conformers of diphosphine.[10-13,15] Theoretical studies carried out on H_2PPH_2 concerned the structure,[22-24,26,28,29,31-33] the conformation analyses,[20,22-24,26,28,29,31] and the possibility of inversion at the P atom.[25,29] Both semiempirical[22,26] and *ab initio*[23,24,26,28,29,31,34] methods predicted the gauche conformer to be the most stable, as far as energy is concerned. Barriers to rotation are contained within 13-20 kJ/mol,[24,26,28,29,31] which implies that such a transformation may be feasible only in certain conditions. On the other hand, inversion at the P atom is unlikely due to the relatively high barrier.[25,29] The above-mentioned study allowed for the estimation of certain energetic,[22-24,26,28,29,31-34,37] thermochemical,[32,35-37] and other[22,28,33] characteristics of diphosphine. Furthermore, some theoretical investigations were focused on the application of both semiempirical[18,21] and *ab initio*[27,30] methods for the interpretation of photoelectron[18] and NMR[21,22,27,30] spectra.

It must be noted, however, that the theoretical studies carried out so far have not considered such essential properties of diphosphine as thermochemical and physicochemical properties, vibrational spectra, and the ability to undergo internal rearrangements and decomposition. Moreover, the relative thermodynamic stability of various forms of diphosphine ought to be re-examined against the background of statistical thermodynamics and advanced quantum chemistry methodology. Lastly, $H_2PPH_2 \rightleftarrows HPPH_3$ tautomerism, important in learning about the possible chemical structures of phosphorus-containing compounds, completes the list of subjects that will be considered in this work.

Methods

Quantum Mechanical Calculations. Quantum mechanical calculations were carried out on a Hewlett-Packard 730 Apollo workstation either on an *ab initio* level using GAMESS,[38] SPARTAN 3.0,[39] and GAUSSIAN 92[40] software or on a semiempirical level employing the MOPAC 93[41] package. Unconstrained geometry optimization of the molecules studied was carried out at the Hartree-Fock (HF) level (restricted (R) in the case of a closed shell or unrestricted (U) for open-shell systems) using gradient techniques.[42,43] The *ab initio* methods employing the STO-3G,[44,45] 4-31G,[46] 6-31G** (6-31G(d,p)),[47,48] DZV,[49] and DZP[50] basis sets implemented in GAMESS, as well as semiempirical MNDO,[51] AM1,[52] and PM3[53] methods incorporated in MOPAC 93, were used to evaluate wave functions. After each optimization was completed, energy Hessian was calculated and checked for positive definiteness, in order to assess whether the structures were true minima.

The propensity of molecules for inversion or rotation, as well as decomposition into smaller fragments, was examined by exploring potential energy surfaces. The energy changes upon rotation around the P-P bond were studied by gradually increasing the HP-PH dihedral angle and carrying out optimization, for each value of the angle, of the remaining internal coordinates on the RHF/6-31G** level.[47,48]

The geometries and energies of the molecules in the transition states were optimized by the gradient minimization technique[42] on the RHF/6-31G** level. After a transition state was optimized, the corresponding energy Hessian always had one and only one negative eigenvalue that indicated a first-order transition state that may point to a true reaction path. The harmonic vibrational frequencies were derived on the basis of numerical values of second derivatives.[54]

Thermodynamic Quantities. The energies of formation ($\Delta_f E$) of the species examined (uncorrected for the zero-point vibrational energy) were calculated following Hess's Law, *i.e.*, subtracting from the energies of gaseous entities the energies of gaseous H_2 and P in the lowest electronic states (multiplied by the relevant stoichiometric coefficients). The quality of thermodynamic quantities[54] was improved by supplementing the RHF (UHF)/6-31G** results with the second-(MP2) and fourth-(MP4) order Møller-Plesset electron correlation correction[55,56] (relevant values are referred to as MP4/6-31G** || RHF/6-31G**, where "||" means "at the geometry of") or by using a quadratic configuration interaction with single and double substitutions and triples contribution (QCISD(T)) together with 6-311+G(3df,2p) and 6-311++G(3df,3pd)

(21) Cowley, A. I.; White, W. D. *J. Am. Chem. Soc.* **1969**, *91*, 1913, 1917.
(22) Cowley, A. H.; White, W. D.; Damasco, M. C. *J. Am. Chem. Soc.* **1969**, *91*, 1922.
(23) Robert, J. B.; Marsmann, H.; Van Wazer, J. R. *J. Chem. Soc., Chem. Commun.* **1970**, 356.
(24) Wagner, E. L. *Theor. Chim. Acta* **1971**, *23*, 127.
(25) Rauk, A.; Andose, J. D.; Frick, W. G.; Tang, R.; Mislow, K. *J. Am. Chem. Soc.* **1971**, *93*, 6507.
(26) Absar, I.; Robert, J.-B.; Van Wazer, J. R. *J. Chem. Soc., Faraday Trans. 2* **1972**, *68*, 799.
(27) Albrand, J. P.; Faucher, H.; Gagnaire, D.; Robert, J. B. *Chem. Phys. Lett.* **1976**, *38*, 521.
(28) Ahlrichs, R.; Heinzmann, R.; Zirz, C. *Theor. Chim. Acta* **1976**, *43*, 29.
(29) Cowley, A. H.; Mitchell, D. J.; Whangbo, M.-H.; Wolfe, S. *J. Am. Chem. Soc.* **1979**, *101*, 5224.
(30) Jansen, H. B.; Meeuwis, A.; Pyykko, P. *Chem. Phys.* **1979**, *38*, 173.
(31) Magnusson, E. *Aust. J. Chem.* **1986**, *39*, 735.
(32) Schiffer, H.; Ahlrichs, R.; Haser, M. *Theor. Chim. Acta* **1989**, *75*, 1.
(33) Korkin, A. A.; Tsvetkov, E. N. *Zh. Neorg. Khim.* **1989**, *34*, 290.
(34) Warren, D. S.; Gimarc, B. M. *J. Am. Chem. Soc.* **1992**, *114*, 5378.
(35) Curtiss, L. A.; Jones, C.; Trucks, G. W.; Raghavachari, K.; Pople, J. A. *J. Chem. Phys.* **1990**, *93*, 2537.
(36) Curtiss, L. A.; Raghavachari, K.; Trucks, G. W.; Pople, J. A. *J. Chem. Phys.* **1991**, *94*, 7221.
(37) Leroy, G.; Temsamani, D. R.; Wilante, C.; Dewispelaere, J.-P. *J. Mol. Struct.: THEOCHEM* **1994**, *309*, 113.
(38) Dupuis, M.; Spangler, D.; Wendoloski, J. J. *National Resource for Computations in Chemistry Software Catalog*; University of California: Berkeley, CA, 1980 (Program QG 01). Current version: Schmidt, M. W.; Baldridge, K. K.; Boatz, J. A.; Jensen, J. H.; Koseki, S.; Gordon, M. S.; Nguyen, K. A.; Windus, T. L.; Elbert, S. T. *QCPE Bull.* **1990**, *10*, 52.
(39) Available from Wavefunction, Inc., 18401 Von Karman, Suite 370, Irvine, CA 92715.
(40) Frisch, M. J.; Trucks, G. W.; Schlegel, H. B.; Gill, P. M. W.; Johnson, B. G.; Wong, M. W.; Foresman, J. B.; Robb, M. A.; Head-Gordon, M.; Replogle, E. S.; Gomperts, R.; Andres, J. L.; Raghavachari, K.; Binkley, J. S.; Gonzales, C.; Martin, R. L.; Fox, D. J.; Defrees, D. J.; Baker, J.; Stewart, J. J. P.; Pople, J. A.; *Gaussian 92/DFT*, Revision F.2; Gaussian, Inc.: Pittsburgh, PA, 1993.
(41) Stewart, J. P. P. *MOPAC 93*; Copyright Fujitsu: Tokyo, Japan, 1993.
(42) Pulay, P. In *Modern Theoretical Chemistry. Vol. 4: Applications of Electronic Structure Theory*; Schaeffer, H. F., III, Ed.; Plenum Press: New York, 1977; pp 153-185.
(43) Schlegel, H. B. *J. Comput. Chem.* **1982**, *3*, 214.
(44) Hehre, W. J.; Stewart, R. F.; Pople, J. A. *J. Chem. Phys.* **1969**, *51*, 2657.
(45) Pople, J. A. *Acc. Chem. Res.* **1970**, *3*, 217.
(46) Ditchfield, R.; Hehre, W. J.; Pople, J. A. *J. Chem. Phys.* **1971**, *54*, 724.
(47) Hariharan, P. C.; Pople, J. A. *Theor. Chim. Acta* **1973**, *28*, 213.
(48) Francl, M. M.; Pietro, W. J.; Hehre, W. J.; Binkley, J. S.; Gordon, M. S.; DeFrees, D. J.; Pople, J. A. *J. Chem. Phys.* **1982**, *77*, 3654.
(49) Dunning, T. H. *J. Chem. Phys.* **1970**, *53*, 2823.
(50) Dunning, T. H. *J. Chem. Phys.* **1989**, *90*, 1007.
(51) Dewar, M. J. S.; Thiel, W. *J. Am. Chem. Soc.* **1977**, *99*, 1285.
(52) Dewar, M. J. S.; Zoebisch, E. G.; Healy, E. F.; Stewart, J. P. P. *J. Am. Chem. Soc.* **1985**, *107*, 3902.
(53) Stewart, J. J. P. *J. Comput. Chem.* **1989**, *10*, 209, 221.
(54) Hehre, W. J.; Radom, L.; Schleyer, P. v. R.; Pople, J. A. *Ab initio Molecular Orbital Theory*; Wiley: New York, 1986.
(55) Møller, C.; Plesset, M. S. *Phys. Rev.* **1934**, *46*, 618.
(56) Krishnan, R.; Frisch, M. J.; Pople, J. A. *J. Chem. Phys.* **1980**, *72*, 4244.

Table 1. Theoretical and Experimental Geometric Parameters of H_2PPH_2 and $HPPH_3$

parameter[a]	theoretical (basis set) MNDO	AM1	PM3	RHF/STO-3G	RHF/4-31G	RHF/DZV	RHF/DZP	RHF/6-31G**	MP4/6-31G**	experimental[b]
					H_2PPH_2 (gauche)					
$r(P_{(1)}-P_{(2)})$				2.175	2.354	2.342	2.214	2.214	2.225	2.218*, 2.219**
$r(P_{(1)}-H_{(11)})$				1.380	1.435	1.420	1.404	1.403	1.410	1.451*, 1.416**
$\angle H_{(11)}P_{(1)}H_{(12)}$				93.5	94.9	96.2	95.6	95.8	94.6	91.3*, 92.0**
$\angle H_{(11)}P_{(1)}P_{(2)}H_{(22)}$				77.0	79.8	79.4	77.5	77.3	77.3	81.0*, 74.0**
					H_2PPH_2 (staggered)					
$r(P_{(1)}-P_{(2)})$	2.023	1.990	2.125	2.178	2.383	2.365	2.232	2.231	2.245	
$r(P_{(1)}-H_{(11)})$	1.340	1.393	1.335	1.381	1.435	1.421	1.406	1.405	1.413	
$\angle H_{(11)}P_{(1)}H_{(12)}$	97.1	97.2	98.8	93.4	94.3	95.4	94.4	94.6	93.3	
$\angle H_{(11)}P_{(1)}P_{(2)}H_{(22)}$	180.0	180.0	180.0	180.2	180.1	180.2	180.2	180.2	179.9	
					$HPPH_3$					
$r(P_{(1)}-P_{(2)})$	1.977	1.639	1.961	2.220	2.358	2.353	2.108	2.117	2.099	
$r(P_{(1)}-H_{(11)})$	1.332	1.376	1.367	1.390	1.460	1.439	1.414	1.413	1.417	
$r(P_{(2)}-H_{(21)})$	1.348	1.238	1.238	1.381	1.417	1.405	1.398	1.397	1.409	
$r(P_{(2)}-H_{(22)})$	1.342	1.238	1.232	1.374	1.410	1.401	1.398	1.389	1.395	
$\angle H_{(21)}P_{(2)}H_{(23)}$	101.1	102.6	100.7	97.7	99.3	101.0	99.4	99.8	97.8	
$\angle H_{(21)}P_{(2)}H_{(22)}$	103.1	102.6	103.6	98.6	100.0	101.3	101.2	101.4	100.5	
$\angle H_{(11)}P_{(1)}P_{(2)}$	102.2	180.0	107.2	87.9	89.0	90.2	91.1	90.2	89.6	
$\angle H_{(11)}P_{(1)}P_{(2)}H_{(22)}$	180.0		180.0	180.0	180.0	180.0	180.0	180.0	179.5	

[a] For the geometry of the molecules and the numbering of the atoms, see Figure 1. Bond lengths (r) are in angstroms and angles ($\angle$) are in degrees. [b] Values with one asterisk arise from electron diffraction studies,[15] while values with two asterisks arise from examination of microwave spectra.[16]

basis sets,[57] eventually with an isogyric correction.[58] This latter correction was assumed to be 3 times ($^1/_2$ times for each unpaired electron on P) the difference between the theoretical and experimental (equal to 458.17 kJ/mol[58]) dissociation energy of the H_2 molecule.

The enthalpies ($\Delta_{f,298}H$) and free enthalpies ($\Delta_{f,298}G$) of formation were obtained in a fashion similar to the derivation of Δ_fE values,[58] using the built-in MOPAC, GAMESS, and GAUSSIAN statistical-mechanics routines. This also allowed for the calculation of other thermodynamic functions, such as entropies ($_{298}S$) and heat capacities ($_{298}C_p$). These values correspond to the gaseous state of all species at a pressure of 1 atm. To bring $\Delta_{f,298}H$ to standard conditions in the usual sense (relevant values are referred to as $\Delta_{f,298}H^{\ominus}$), the enthalpy of P was lowered by 316.5 kJ/mol, *i.e.*, the enthalpy of atomization.[59,60] To obtain free enthalpies of formation in standard conditions, the theoretically determined entropy of P was lowered by 122.1 kJ/mol K, *i.e.*, the difference in entropy of the species in gaseous and solid state, respectively.[59,60]

Effect of Temperature on Equilibria and Kinetics of Decomposition. The influence of temperature on equilibria between tautomeric forms or conformations (tr), as well as reactants upon decomposition (d), was examined following the equation

$$K_a = \exp[-\Delta_{tr(d)}G/(RT)] \quad (1)$$

where R is the gas constant, T is the temperature, and K_a is the thermodynamic equilibrium constant, while $\Delta_{tr(d)}G$ results from Gibbs equation

$$\Delta_{tr(d)}G = \Delta_{tr(d)}H - \Delta_{tr(d)}(TS) \quad (2)$$

All thermodynamic data required for these calculations were computed as described in the previous section. Energy changes for all processes corresponded to the QCISD(T)/6-311+G(3df,2p) level and RHF/6-31G** geometries.

The high-pressure-limit rate constants ($k_\infty(T)$) for the unimolecular processes were calculated employing the RRKM theory.[61]

$$k_\infty(T) = \frac{L^+}{NhQ_v}\exp\left(-\frac{E_0}{RT}\right)\int_0^\infty P(E^+_v)\exp\left(-\frac{E^+_v}{RT}\right)dE^+_v \quad (3)$$

where N and h represent Avogadro's number and Planck's constant, respectively, Q_v is the vibrational partition function, L^+ is the reaction path degeneracy, E_0 is the critical energy (the difference in energy between the transition and ground state of the molecule), E^+_v is the excess of energy above E_0, and $P(E^+_v)$ is the density of vibrational states of the molecule in the transition state relevant to a given level of energy (E^+_v) (evaluated on the basis of the Whitten–Rabinovitch approximation,[62] using calculated frequencies).

Results and Discussion

Geometry and Energetics. The structural parameters characterizing the molecules investigated calculated at various levels of theory are summarized in Table 1, whereas energetic and thermochemical characteristics are shown in Tables 2 and 3. The results obtained in DZV, DZP, and 6-31G** basis sets reveal that diphosphine is energetically more stable in the gauche conformation than in the staggered conformation (Table 2, Figure 1), while in less extensive *ab initio* basis sets, the staggered conformation appears more stable. All three semiempirical methods indicate that diphosphine exists only in a staggered conformation (Table 3). The findings resulting from advanced *ab initio* methods conform with the experimental ones that indicate that diphosphine exists predominantly in the gauche conformation. The existence of such a form has been revealed from electron diffraction[15] and IR–microwave[16] studies, as well as comparison of experimental photoelectron[18] and ^{31}P-NMR[13,21,27] spectra with theoretical ones. Therefore, optimizations on the DZV, DZP, and 6-31G** levels seem to reflect well the geometry and energetics of the molecules studied. Among the basis sets implemented in this work, DZP and 6-31G** appear to be the most adequate since they always afforded structural parameters that compared well with the experimental ones. For these reasons, most of the calculations refer to the 6-31G** basis set. The corresponding energies were

(57) Foresman, J. B.; Frisch, A. *Exploring Chemistry with Electronic Structure Methods: A Guide to Using Gaussian*; Gaussian, Inc.: Pittsburgh, PA, 1993.
(58) Pople, J. A.; Luke, B. T.; Frisch, M. J.; Binkley, J. S. *J. Phys. Chem.* **1985**, *89*, 2198.
(59) CODATA recommended key values for thermodynamics: *J. Chem. Thermodyn.* **1978**, *10*, 903.
(60) *Handbook of Chemistry and Physics*, 73rd ed.; Lide, D. R., Ed.; CRC Press: Boca Raton, FL, 1992–1993.
(61) Robinson, P. J.; Holbrook, K. A. *Unimolecular Reactions*; Wiley: London, 1972.
(62) Whitten, G. Z.; Rabinovitch, B. S. *J. Chem. Phys.* **1963**, *38*, 2466.
(63) Hartley, S. B.; Holmes, W. S.; Jacques, J. K.; Mole, M. F.; McCoubrey, J. C. *Q. Rev., Chem. Soc.* **1963**, *17*, 204.
(64) Wagman, D. D.; Evans, W. H.; Parker, V. B.; Schumm, R. H.; Halow, I.; Bailey, S. M.; Churney, K. L.; Nutall, R. L. *J. Phys. Chem. Ref. Data, Suppl.* **1982**, *11*, No. 2.

Table 2. Total Energies (in hartrees) of the Gauche Conformation of H_2PPH_2 and Energies of Other Forms (in kJ/mol) Relative to This, at Various Levels of Theory[a]

	H_2PPH_2		
basis set||geometry	gauche	staggered	$HPPH_3$
RHF/STO-3G||RHF/STO-3G	−676.140 10	−3.7	290.6
MP2/STO-3G||RHF/STO-3G	−676.210 64	−5.1	300.8
MP4/STO-3G||RHF/STO-3G	−676.238 72	−5.8	304.6
RHF/4-31G||RHF/4-31G	−682.921 53	−1.0	156.3
MP2/4-31G||RHF/4-31G	−683.039 31	−2.7	164.1
MP4/4-31G||RHF/4-31G	−683.071 35	−3.5	166.1
RHF/DZV||RHF/DZV	−683.654 42	2.1	129.9
MP2/DZV||RHF/DZV	−683.780 22	−0.7	132.4
MP4/DZV||RHF/DZV	−683.812 90	−1.8	133.1
RHF/DZP||RHF/DZP	−683.757 54	3.6	126.3
MP2/DZP||RHF/DZP	−683.998 02	2.2	114.9
MP4/DZP||RHF/DZP	−684.045 31	1.5	118.5
RHF/6-31G**||RHF/6-31G**	−683.760 50	4.4	122.1
MP2/6-31G**||RHF/6-31G**	−683.991 37	3.2	111.4
MP4/6-31G**||RHF/6-31G**	−684.038 06	2.4	115.0
MP4/6-31G**||MP4/6-31G**	−684.038 22	2.1	114.2
QCISD(T)/6-311+G(3df,2p)||RHF/6-31G**	−684.185 59	2.0	98.9
QCISD(T)/6-311++G(3df,3pd)||RHF/6-31G**	−684.196 49	2.1	98.6

[a] Literature *ab initio* data for diphosphine (total energy in hartrees), energy difference between staggered and gauche conformations (in kJ/mol): −677.679 15, −0.6 (Gaussian type orbitals);[24] −682.4850, 2.1 (Gaussian type orbitals);[23] −682.907 15, −0.1 (4-31G);[29] −683.011 73, 0.1 (4-31G);[31] −683.0385, 0.8 (4-31G*);[34] −683.664 14, 6.3 (Gaussian type orbitals);[27] −683.738 04, 2.3 (DZP);[34] −683.7605, 4.5 (6-31G**);[34] −684.014 58 (MP2/6-31G**\|\|MP2/6-31G**);[37] −684.099 15 (G1 theory);[35] −684.183 62 (SDTQ/6-311++G(3df,2p)\|\|MP2/6-31G**);[37] −684.186 88 (G2 theory).[36]

Table 3. Thermodynamic Characteristics of Gaseous H_2PPH_2 and $HPPH_3$ at Various Levels of Theory

	H_2PPH_2[a]								$HPPH_3$[a]			
	gauche				staggered							
method or basis set||geometry	$\Delta_{f,298}H^{\ominus}$ [b]	$\Delta_{f,298}G^{\ominus}$	$_{298}S^{\ominus}$	$_{298}C_p^{\ominus}$	$\Delta_{f,298}H^{\ominus}$ [b]	$\Delta_{f,298}G^{\ominus}$	$_{298}S^{\ominus}$	$_{298}C_p^{\ominus}$	$\Delta_{f,298}H^{\ominus}$	$\Delta_{f,298}G^{\ominus}$	$_{298}S^{\ominus}$	$_{298}C_p^{\ominus}$
MNDO					−12.0		271.6	59.8	211.1		274.1	64.0
AM1					27.6		271.6	61.9	-27.1		266.6	56.5
PM3					−11.0		285.0	68.2	-38.2		272.0	63.2
RHF/DZP||RHF/DZP	342.7	357.5	269.4	57.9	346.0	358.6	276.7	58.4	470.2	485.8	266.7	57.6
	(31.7)	(46.5)			(35.1)	(47.7)			(159.2)	(174.8)		
MP4/DZP||RHF/DZP	159.1	173.9			160.3	172.9			278.7	294.3		
	(114.4)	(129.2)			(115.6)	(128.2)			(234.1)	(249.7)		
RHF/6-31G**||RHF/6-31G**	340.3	355.1	269.4	58.1	344.3	356.5	278.1	58.6	463.9	479.4	267.1	57.8
	(28.6)	(43.4)			(32.7)	(44.9)			(152.2)	(167.7)		
MP4/6-31G**||RHF/6-31G**	169.9	184.7			172.1	184.3			286.4	301.9		
	(120.2)	(135.0)			(122.3)	(134.5)			(236.7)	(252.2)		
MP4/6-31G**||MP4/6-31G**	169.2	184.0			171.0	183.2			284.9	300.4		
	(118.9)	(133.7)			(120.7)	(132.9)			(234.6)	(250.1)		
QCISD(T)/6-311+G(3df,2p)||RHF/6-31G**	74.9	89.7			76.6	88.8			175.4	190.9		
	(49.2)	(64.0)			(50.9)	(63.1)			(149.6)	(165.1)		
QCISD(T)/6-311++G(3df,3pd)||RHF/6-31G**	55.3	70.1			57.0	69.2			155.4	170.9		
	(42.9)	(57.7)			(44.7)	(56.8)			(143.0)	(158.5)		

[a] $\Delta_{f,298}H^{\ominus}$ and $\Delta_{f,298}G^{\ominus}$ values in kilojoules per mole; $_{298}S^{\ominus}$ and $_{298}C_p^{\ominus}$ values in joules per mole per kelvin (values in parentheses have included isogyric correction). [b] Literature values of the standard enthalpy of formation of gaseous diphosphine (in kJ/mol) are 49.7 (value 20.9 reported in ref 7 and widely cited following this reference,[2,60,63,64] evaluated on the basis of calorimetrically measured heat of explosive decomposition of the hydride, most probably relates to the liquid state of H_2PPH_2, and the value mentioned above is obtained by adding the enthalpy of vaporization equal to 28.8[2,6]) and 41.4 (value derived from the appearance potentials[8]).

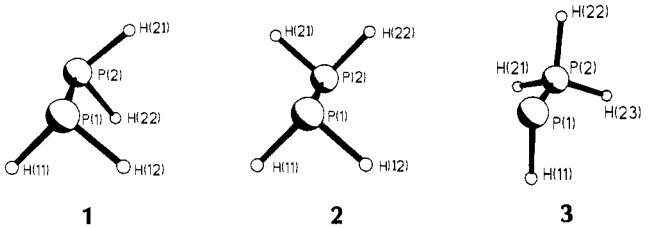

1 2 3

Figure 1. Structures of H_2PPH_2 and $HPPH_3$ optimized at MP4/6-31G** level.

also calculated for the 6-31G** geometries. The complete geometry optimizations at the 6-31G** level with fourth-order electron correlation included only a slight change of geometry (Table 1) and energy lower by ca. 0.4 kJ/mol (Table 2). As the latter calculations are very time-consuming, they were carried out for only some selected low-energy structures.

Values of the $H_{(11)}P_{(1)}P_{(2)}H_{(21)}$ dihedral angle (Figure 1) for the gauche conformation of diphosphine, determined at the RHF/DZP, RHF/6-31G**, and MP4/6-31G** levels, fall exactly between those arising from the experiment.[15,16] The values of this angle predicted in earlier calculations (in degrees, 75,[24,26] 76,[29] 76−78,[28] 77,[31] and 77.7[32]) are close to each other, although only those from the recent papers cited compare well with ours. Other structural parameters determined here also compare well with the experimental ones, which implies that the theory correctly predicts the geometry of the molecules studied.

All *ab initio* calculations reveal that the $HPPH_3$ molecule should have a much higher energy (*i.e.*, should be much less stable thermodynamically) than H_2PPH_2. The energy difference between these tautomeric forms decreases when performing more advanced calculations (Table 2). Among semiempirical methods, only MNDO results are qualitatively comparable with *ab initio* ones. AM1 and PM3 predict $HPPH_3$ to have a lower energy than H_2PPH_2 (Table 3). No comparison of theoretical

Table 4. Kinetic (K) and Thermodynamic (Th) Barriers for Structural Transformations (tr) in H_2PPH_2 and $HPPH_3$ Relevant to 6-31G** Geometries

		quantity[a]									
		$\Delta_{tr}E$			$\Delta_{tr,298}H^{\ominus}$			$\Delta_{tr,298}G^{\ominus}$			
transition/molecule (states)	type of barrier	RHF	MP4	QCISD(T)/ 6-311+G(3df,2p)	RHF	MP4	QCISD(T)/ 6-311+G(3df,2p)	RHF	MP4	QCISD(T)/ 6-311+G(3df,2p)	$\Delta_{tr,298}S^{\ominus}$
rotation/H_2PPH_2 (gauche−gauche)	K	19.5	19.1	17.5	16.6	16.2	14.6	18.8	18.5	16.8	−7.6
rotation/H_2PPH_2 (gauche−staggered)	Th	4.4	2.4	2.0	4.1	2.2	1.7	1.4	−0.5	−0.9	8.7
	K	5.3	3.7	3.2	2.9	1.3	0.8	5.2	3.6	3.1	−7.9
rotation/$HPPH_3$	K	9.9	11.3	8.6	7.3	8.7	5.9	9.0	10.5	7.7	−6.0
inversion/H_2PPH_2 (gauche−gauche)	K	122.4	117.8	111.0	119.1	114.5	107.6	120.6	115.9	109.1	−4.9
unimolecular tautomerization/	Th	122.1	115.0	98.9	123.6	116.5	100.5	124.3	117.2	101.2	−2.3
H_2PPH_2−$HPPH_3$	K	339.6	272.6	253.7	329.8	262.8	243.9	331.6	264.6	245.6	−6.0

[a] $\Delta_{tr}E$, $\Delta_{f,298}H^{\ominus}$ and $\Delta_{f,298}G^{\ominus}$ values in kilojoules per mole; $\Delta_{tr,298}S^{\ominus}$ values in joules per mole per kelvin. $\Delta_{tr,298}H^{\ominus}$, $\Delta_{tr,298}G^{\ominus}$, and $\Delta_{tr,298}S^{\ominus}$ values for transition states (kinetic barriers) correspond to the partition function contributions calculated using all normal frequencies except the imaginary frequency, which is associated with the reaction path.

and experimental geometries of $HPPH_3$ is feasible due to the lack of experimental information in this matter. Detailed analysis of the parameters compiled in Table 1, corresponding to various levels of theory, reveals relatively large differences in the values of the $H_{(11)}P_{(1)}P_{(2)}$ valence angle. The *ab initio* methods predict this angle to be close to the right angle, while AM1 predicts this angle to be close to the linear angle (which means that the $H_{(11)}$, $P_{(1)}$, and $P_{(2)}$ atoms are located on one line). In view of the earlier discussion, however, semiempirical methods do not correctly predict the energetics of phosphorus hydrides; thus, the geometry obtained using these methods cannot be considered reliable. It can therefore be concluded that the $HPPH_3$ molecule, if existing, would most probably assume a geometry similar to that determined by the *ab initio* methods.

Thermochemistry. Enthalpies and free enthalpies of formation, as well as entropies and heat capacities, of gaseous H_2PPH_2 and $HPPH_3$ are shown in Table 3. Most of these characteristics have not previously been known. Only the enthalpies of formation can be compared with values originating from the experiment. The most appropriate for such a comparison are characteristics determined without an isogyric correction. $\Delta_{f,298}H^{\ominus}$ for the gauche diphosphine relevant to the most advanced level of theory equals 55.3 kJ/mol and somewhat exceeds experimental heats of formation (Table 3). The isogyric correction is, in this case, relatively small and leads to the improvement of conformity between theoretical and experimental data. Trends observed upon examining data in Table 3 seem to indicate that the use of basis sets more advanced than 6-31G** for geometry optimizations could further increase conformity between both sets of characteristics. Such calculations were, however, beyond our possibilities.

It is worth mentioning that energies of P, H_2, and H_2PPH_2 have recently been determined employing G-1 (Gaussian-1) and G-2 theories.[36] Using these data, one obtains Δ_fE values (in kJ/mol) equal to −576.0 and −572.0, respectively (with high level correction instead of isogyric correction). Adding subsequently the enthalpy of atomization of P and a term accounting for the enthalpy difference between the standard state and the isolated species gives standard enthalpies of formation of diphosphine equal to 72.8 (G-1) and 76.8 (G-2). These values differ much more from the experimental heats of formation than the best of our results.

Another possibility of determining heats of formation of entities containing more than one phosphorus atom would be the theoretical determination of heats of hydrogenation reaction (*e.g.*, $H_2PPH_2 + H_2 \rightarrow 2PH_3$) and combination of these with the heat of formation of phosphine.[37,65] Such a procedure does not seem applicable in our case, since experimental heats of formation of PH_3 are fairly scattered (5.4,[7] 7.1,[58] 9.2,[66,67] and 9.6[67] kJ/mol) and thus not sound as reference values.

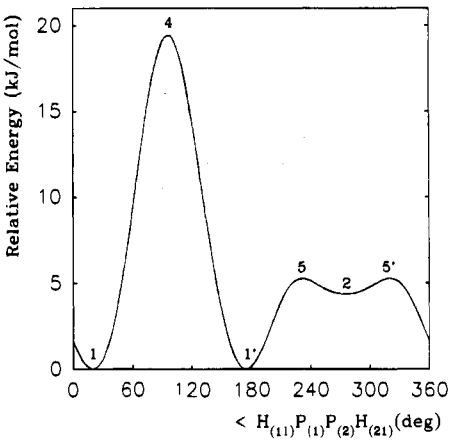

Figure 2. Energy of H_2PPH_2 relative to that of the lowest energy structure (**1** in Figure 1) upon rotation around the P−P bond at the RHF/6-31G** level (numbers indicate structures in Figures 1 and 3 or structures being their mirror images).

The data in Table 3 reveal that the less advanced the basis set used, the higher the enthalpies of formation. $\Delta_{f,298}H^{\ominus}$ values derived on the DZP or 6-31G** level exceed 340 kJ/mol and are thus unrealistic when compared with experimental characteristics. In the case of these two basis sets, the very high isogyric correction brings enthalpies of formation to acceptable values. The introduction of such a substantial correction, however, gives rise to questions as to the reliability of the characteristics obtained. It seems more adequate to consider the magnitude of this correction as an indicator of the soundness of the choice of the basis set; namely, the lower the isogyric correction, the better the basis set.

The differences in both enthalpies and free enthalpies of formation between staggered and gauche conformers of diphosphine decrease if more advanced calculations are performed (Tables 3 and 4). The values of $\Delta_{tr,298}G^{\ominus}$ even become negative (Table 4), which implies that a staggered form is thermodynamically preferred rather than a gauche one. This results from the fact that although enthalpy acts in favor of the gauche form (positive $\Delta_{tr,298}H^{\ominus}$), the entropy favors more symmetric staggered molecules (positive $\Delta_{tr,298}S^{\ominus}$). This is illustrated in Figure 2, where relative energies are plotted against the $H_{(11)}P_{(1)}P_{(2)}H_{(21)}$ dihedral angle in H_2PPH_2.

(65) Sana, M.; Leroy, G. *Ann. Soc. Sci. Bruxelles, Ser. I* **1991**, *105*, 67.
(66) *National Bureau Standard Circular 500*; U. S. Government Printing Office: Washington, DC, 1949, 1952, 1958 (following ref 67).
(67) Saalfeld, F. E.; Svec, H. J. *Inorg. Chem.* **1963**, *2*, 46.
(68) Wada, Y.; Kiser, R. W. *Inorg. Chem.* **1964**, *3*, 174.

Table 5. Physicochemical Characteristics[a]

	H_2PPH_2[b]						$HPPH_3$		
	gauche			staggered					
	dipole	energy		dipole	energy		dipole	energy	
method or basis set||geometry	moment	HOMO	LUMO	moment	HOMO	LUMO	moment	HOMO	LUMO
MNDO				0.0	−10.314	−0.327	5.45	−7.723	−1.268
AM1				0.0	−9.872	−0.252	3.30	−11.370	0.503
PM3				0.0	−7.860	−0.818	7.10	−7.708	−0.176
RHF/DZP||RHF/DZP	1.25	−9.870	3.780	0.0	−9.146	3.633	4.20	−7.470	3.548
RHF/6-31G**||RHF/6-31G**	1.39	−9.826	3.448	0.0	−9.086	3.325	4.49	−7.437	3.336
MP4/6-31G**||MP4/6-31G**	1.35	−9.878	3.374	0.0	−9.200	3.233	4.27	−7.510	3.265
RHF/6-311+G(3df,2p)||RHF/6-31G**	1.17	−9.847	1.500	0.0	−9.113	1.499	4.17	−7.600	1.111
RHF/6-311++G(3df,3pd)||RHF/6-31G**	1.18	−9.845	1.121	0.0	−9.110	1.127	4.18	−7.603	0.857

[a] Dipole moment values in debye; energies of HOMO and LUMO in electronvolts. [b] Values of the dipole moment and the ionization potential of diphosphine determined theoretically amount to 3.22 D and 9.20 eV, respectively.[22] Values of the ionization potential derived from the appearance potentials range from 8.7 to 10.6 eV,[8,9,68] while that from photoelectron spectra equals 9.69 eV[18] (according to Koopmans' theorem,[69] the energies of the highest occupied (HOMO) and the lowest unoccupied (LUMO) molecular orbitals, multiplied by −1, represent, in the first approximation, the ionization potential and electron affinity of a molecule, respectively.)

Physicochemical Characteristics. As semiempirical methods do not correctly predict the geometry and energetics of diphosphines, the physicochemical characteristics calculated by these cannot be reliable (Table 5). The following discussion will therefore be focused only on the data determined on the *ab initio* level.

The H_2PPH_2 in the staggered conformation is nonpolar since the molecule has a center of symmetry, while in the gauche conformation it is slightly polar, owing to the lack of such an element of symmetry. $HPPH_3$, if existing, would exhibit a relatively high polarity, manifested by a dipole moment higher than 4 D.

The ionization potential (IP) (opposite in value to the energy of HOMO[69]) is predicted higher for the gauche form than for the staggered form of H_2PPH_2. The values of this quantity for both forms comprise, however, between 8.7 and 10.6 eV, the range that has been extracted from appearance potentials[8,9,68] and photoelectron spectra.[18] It appears, therefore, that the experimental values fit equally well to the theoretically determined ionization potentials for both gauche and staggered forms. It can also be noted that theory predicts lower IP values for $HPPH_3$ molecules than for H_2PPH_2 molecules.

The electron affinity (EA) (energy change accompanying the electron attachment, which can be approximated by a value opposite to LUMO energy[69]) of diphosphines is predicted to be negative in all cases, which implies that the process is energetically favored. The theoretical EA values are similar for both conformers of H_2PPH_2 and somewhat lower than those of $HPPH_3$. This suggests that H_2PPH_2 would form more stable negative ions than $HPPH_3$.

Vibrational Transitions. The harmonic vibrational frequencies (and intensities) determined at the 6-31G** level are shown, together with experimental data, in Table 6. This table also presents scaled frequencies, which were obtained by multiplying theoretical values by the factor 0.889, derived in this paper (see footnote to Table 6). Multiplication of frequencies by such a factor (typically 0.89) is commonly required, if frequencies obtained from 6-31G** basis set are to be compared with those resulting from experiment.[57]

Vibrational frequencies calculated for $HPPH_3$ have only theoretical significance, as the existence of such a molecule has not, to our knowledge, been demonstrated. On the other hand, scaled theoretical frequencies can be compared with real absorption spectra of diphosphine. This comparison reveals that the theoretical frequencies of both gauche and staggered H_2PPH_2 correlate equally well with the experimental spectra. The only substantial difference in frequencies of both forms concerns the region of rocking (torsion) vibrations. For the gauche conformer, this vibration should occur at 206 cm^{-1} (experimental, 217 cm^{-1}), while for the staggered conformer, this vibration should occur at 79 cm^{-1} (absorption in this region has been noted and ascribed to lattice vibrations[14,17]). It is, therefore, evident from the comparison of experimental and theoretical transitions that both conformers of H_2PPH_2 can participate in the absorption of infrared radiation. This observation creates a basis for changing our point of view concerning the structure of one of the simplest phosphorus hydrides, H_2PPH_2.

Structural Transformations. Two types of structural transformations are essential for H_2PPH_2, namely rotation around the P−P bond and inversion at the P atom. Energy change upon rotation is shown in Figure 2, and transition state structures for both rotation and inversion are shown in Figure 3. Further, Table 4 includes thermodynamic and kinetic barriers to structural transformations, and Table 7 includes thermodynamic characteristics of the transition states for such processes. Complete rotation in H_2PPH_2 would require overcoming an energy barrier of as high as 17.5 kJ/mol (the free enthalpy barrier would be 16.8 kJ/mol, considering data arising from QCISD(T)/6-311+G(3df,2p)) (Table 4), which is not likely to be passed at room temperature. On the other hand, the kinetic energy barrier to the transition between the gauche and the staggered conformations equals 3.2 kJ/mol and exceeds the thermodynamic energy barrier by only 1.2 kJ/mol. The behavior of H_2PPH_2 molecules on the macroscopic scale, however, acts in favor of the staggered form, which is manifested by an increase of entropy and a decrease of excess enthalpy over energy. As a result, the ratio of molecules in staggered/gauche conformation in the gaseous phase increases with temperature (Figure 4), attaining a value of 1 (relevant to $\Delta_f G^\ominus_{staggered} - \Delta_f G^\ominus_{gauche} = 0$) at *ca.* 200 K. At room temperature, this ratio would be 1.46 on the basis of data from Table 4. It can thus be concluded that a mixture of staggered and gauche conformers of H_2PPH_2 can be expected in the gaseous phase at ambient temperature. The ratio of staggered/gauche molecules increases on moving to elevated temperatures. The barrier for complete rotation around the P−P bond in H_2PPH_2 is not likely to be overcome at ambient temperature. The molecule can, however, easily undergo torsional movements between **1** and **1'** states (Figure 2). This is fully confirmed by very low frequencies relevant to such vibrations.

The energy barrier to the inversion at the P atom in H_2PPH_2 is of the order of 111 kJ/mol (free enthalpy barrier equals 109.1

(69) Koopmans, T. *Physica* **1934**, *1*, 104.

Table 6. Harmonic Frequencies (cm^{-1}) and Intensities ($D^2/Å^2$ amu) (in parentheses) Calculated at the RHF/6-31G** Level Together with Experimental Vibrational Frequencies (cm^{-1}) for H_2PPH_2 and $HPPH_3$

H_2PPH_2 (gauche)					
mode[a]		frequency (intensity)			
				observed	
assignment	description	theoretical	scaled[c]	range of value	ref
$\nu_7(a)$	H_2PPH_2 rocking (torsion)	232 (0.072)	206	217	17
$\nu_6(a)$	PP stretching	489 (0.012)	435	433−438	17 and 19
$\nu_{12}(b)$	as-HPP deformation (twisting)	693 (0.426)	616	635−643	14, 17, and 19
$\nu_5(a)$	s-HPP deformation (wagging)	723 (0.261)	643	628−648	17 and 19
$\nu_{11}(b)$	as-HPP deformation (wagging)	926 (1.480)	823	784−882	10, 14, 17, and 19
$\nu_4(a)$	s-HPP deformation (twisting)	973 (0.000)	865	792−872	14, 17, and 19
$\nu_{10}(b)$	as-HPH deformation (scissors)	1228 (1.030)	1092	1052−1081	10, 14, 17, and 19
$\nu_3(a)$	s-HPH deformation (scissors)	1246 (0.443)	1108	1037−1067	17 and 19
$\nu_9(b)$	as-PH stretching	2569 (1.035)	2284	2281−2320	17
$\nu_2(a)$	s-PH stretching[b]	2578 (0.647)	2292	2268	17
$\nu_1(a)$	s-PH stretching[b]	2585 (2.585)	2298	2295−2312	17
$\nu_8(b)$	as-PH stretching	2589 (3.909)	2302	2299	17

H_2PPH_2 (staggered)				
mode[a]		frequency (intensity)		
assignment	description	theoretical	scaled[c]	observed[14]
$\nu_7(a_u)$	H_2PPH_2 rocking (torsion)	79 (0.242)	70	169
$\nu_4(a_g)$	PP stretching	486 (0.000)	432	437
$\nu_6(a_u)$	s-HPP deformation (twisting)	689(0.611)	613	781
$\nu_{12}(b_u)$	as-HPP deformation (wagging)	721 (0.401)	641	636
$\nu_3(a_g)$	s-HPP deformation (wagging)	964 (0.000)	857	653
$\nu_9(b_g)$	as-HPP deformation (twisting)	1008 (0.000)	896	878
$\nu_2(a_g)$	s-HPH deformation (scissors)	1221 (0.000)	1085	1049
$\nu_{11}(b_u)$	as-HPH deformation (scissors)	1224 (1.089)	1088	1053
$\nu_8(b_g)$	as-PH stretching[b]	2560 (0.000)	2276	2281
$\nu_1(a_g)$	s-PH stretching[b]	2566 (0.000)	2281	2281
$\nu_{10}(b_u)$	as-PH stretching[b]	2570 (3.658)	2285	2296
$\nu_5(a_u)$	s-PH stretching[b]	2574 (4.695)	2288	2296

$HPPH_3$			
mode[a]		frequency (intensity)	
assignment	description	theoretical	scaled[c]
$\nu_{12}(a'')$	$HP_{(1)}P_{(2)}H_3$ (torsion)	296 (0.208)	263
$\nu_{11}(a')$	$P_{(1)}P_{(2)}$ stretching	495 (0.202)	440
$\nu_{10}(a')$	s-$HP_{(1)}P_{(2)}H_3$ deformation (wagging)	587 (0.399)	522
$\nu_9(a'')$	as-$P_{(2)}H_3$ deformation (twisting)	691 (0.009)	614
$\nu_8(a')$	s-$HP_{(1)}P_{(2)}H_3$ deformation (wagging)	962 (0.835)	855
$\nu_7(a'')$	as-$P_{(2)}H_3$ deformation (scissors)	1180 (0.580)	1049
$\nu_6(a')$	s-$P_{(2)}H_3$ deformation (inversion)	1195 (4.190)	1062
$\nu_5(a')$	s-$P_{(2)}H_3$ deformation (scissors)	1279 (3.304)	1137
$\nu_4(a')$	s-$P_{(1)}H$ stretching	2509 (2.914)	2231
$\nu_3(a'')$	as-$P_{(2)}H$ stretching[b]	2595 (2.056)	2307
$\nu_2(a')$	s-$P_{(2)}H$ stretching[b]	2619 (3.416)	2328
$\nu_1(a')$	s-$P_{(2)}H$ stretching	2690 (0.792)	2391

[a] Theoretical and also refs 14, 17, and 19; s = symmetric and as = assymetric. [b] Two PH bonds of PH_2 or PH_3 are involved in the stretching mode. [c] Values obtained by multiplying theoretical frequencies (ν_{theor}) by the factor $K = 0.889$, which results from the minimization, with respect to K, of the statistical function $\sum_i\{[(\nu_{theor})_iK - (\nu_{exp})_i]/[(\nu_{theor})_iK]\}^2$ (ν_{exp} denotes the experimental value of frequency and i indicates the frequencies) on the basis of data for the gauche conformation of H_2PPH_2.

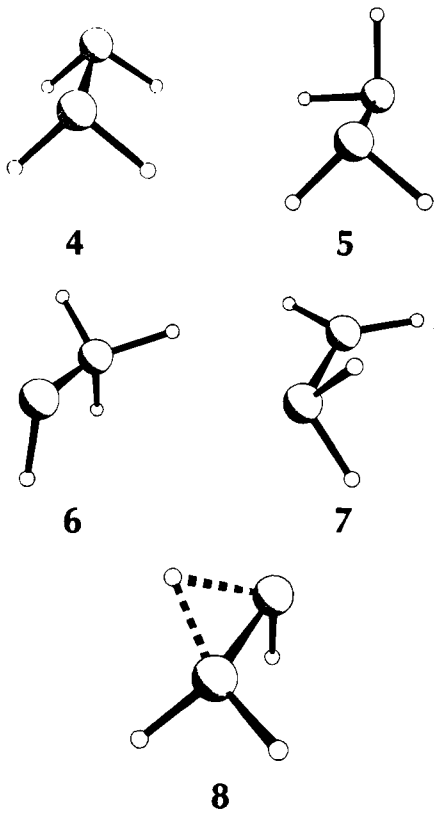

Figure 3. Transition state structures upon rotation between two gauche conformations of H_2PPH_2 (**4** in Figure 2), transfer between gauche and staggered conformations of H_2PPH_2 (**5** in Figure 2), rotation in $HPPH_3$ (**6** in Figure 5), inversion between two gauche conformations of H_2PPH_2 (**7**), and unimolecular hydrogen transfer changing H_2PPH_2 to $HPPH_3$ (**8**).

kJ/mol) (Table 4), which indicates that such a process is not likely to occur even at elevated temperatures. Similar conclusions have been drawn by other authors.[25,29]

Complete rotation around the P−P bond in $HPPH_3$ (Figure 5) exhibits three identical minima corresponding to the same lowest energy structure **3** (Figure 1) and three saddle points corresponding to the same structure **6** (Figure 3). The energy barrier for the process is 8.6 kJ/mol and that of free enthalpy is 7.7 kJ/mol (Table 4) (thermodynamic data for the transition state are given in Table 7), which means that if the $HPPH_3$ molecule existed, it would not be susceptible to this type of structural transformation. On the other hand, this energy barrier is typical for rotation around a single bond, which implies that the P−P bond in $HPPH_3$ exhibits a single bond character. A similar conclusion arises from the analysis of bond lengths summarized in Table 1.

$H_2PPH_2 \rightleftharpoons HPPH_3$ Tautomerization. The $HPPH_3$ molecule exhibits an energy of 98.9 kJ/mol (data relevant to QCISD(T)/6-311+G(3df,2p) level) above that of its tautomeric form H_2PPH_2 (free enthalpy difference is 101.2 kJ/mol) (Table 4). At such a large energy difference, the ratio of the amounts of $HPPH_3/H_2PPH_2$ is predicted to be very small at ambient temperature and increases very slowly with temperature (Figure 6). At a temperature of *ca.* 40 000 K, the equilibrium constant attains 1, which corresponds to equal amounts of both tautomers.

The less energetically stable $HPPH_3$ molecule can be created in either a unimolecular or a bimolecular hydrogen transfer. The transition state for the unimolecular hydrogen transfer (structure **8** in Figure 3), whose thermochemical characteristics are included in Table 7, exhibits an energy of 253.7 kJ/mol above that of the gauche conformer of H_2PPH_2 (the free enthalpy barrier is 245.6 kJ/mol, Table 4). The energy barrier for the reverse process is also relatively high (154.8 kJ/mol, Table 4), which means that once formed, the $HPPH_3$ molecule would exist for a very long time. However, in macroscopic systems, collisions with surrounding molecules allow bimolecular hydrogen transfer to occur. The search for a transition state of such a process (at the RHF/6-31G** level) did not end successfully. It can therefore be concluded that the energy of the transition state between H_2PPH_2 and $HPPH_3$ is very close to that of the latter tautomer, *i.e.*, the second energy minimum is very shallow. Thus, if an $HPPH_3$ molecule were somehow created, it would spontaneously tautomerize to H_2PPH_2 in a bimolecular process.

It can therefore be concluded that $HPPH_3$ is very unlikely to be isolated in measurable amounts (Figure 6). Such a species can only be considered as an intermediate in reactions involving H_2PPH_2.

Behavior of Diphosphines at Elevated Temperatures. As the energy of $HPPH_3$ substantially exceeds that of the gauche conformer of H_2PPH_2 (Tables 2 and 4), the former molecule can occur only at elevated temperatures. In these conditions, however, decomposition of diphosphines or of the products of such processes can take place. The energetic and thermodynamic characteristics of some selected decomposition processes are summarized in Table 8.

Two ways of decomposition of H_2PPH_2 were considered, namely H_2 elimination leading to triplet or singlet PPH_2 (eqs 4 and 5) and P−P bond fission affording two PH_2 radicals (eq 6). In the case of $HPPH_3$, the only process taken into account is dissociation toward PH_3 and singlet or triplet PH (eqs 7 and 8). Further, processes considered are decomposition of PPH_2, formed in reactions 4 and 5 (eqs 9 and 10), and PH_3, expected to be formed in reactions 7 and 8 and other processes not mentioned in Table 8 (eqs 11 and 12). Transition state structures for reactions 4 and 9 are shown in Figure 7.

To gain insight into the behavior of diphosphines at elevated temperatures, it is worth considering the problem from both kinetic and thermodynamic points of view. The high-pressure-limit rate constants for five unimolecular processes (tautomerization, eqs 4, 6, 9, and 11), determined by the RRKM theory, are shown in Figure 8, and Arrhenius parameters are shown in Table 9. Only the rate constants of the decomposition of PH_3 (eq 11) can be compared with values originating from experiment.[70−73] This comparison reveals that in reality, phosphine decomposes much faster than theory predicts (experimental Arrhenius activation barriers are in the 220−240 kJ/mol range[72,73] and thus are substantially lower than those predicted by theory). The rate constants originating from experiments were mostly determined on the basis of measurements of the depletion of PH_3 and thus affected by secondary processes. The theoretical values in Table 9 do not contain such deficiencies. Moreover, since kinetic parameters were derived on the same theoretical bases, they should reflect well mutual relations between various possible processes.

As shown in Figure 8, bond fission in H_2PPH_2 (eq 6) is slightly more likely than H_2 elimination (eq 4). Both processes compete with the transformation of H_2PPH_2 to $HPPH_3$. This means that $HPPH_3$ could never be obtained by heating H_2PPH_2 since the energy that must be supplied to the molecules is sufficient to cause their decomposition. According to the data

(70) Blazejowski, J.; Lampe, F. W. *XIII International Conference on Photochemistry*; Abstracts, Vol. II; Budapest, Hungary, 1987; p 520.
(71) Buchan, N. J.; Jasinski, J. M. *J. Cryst. Growth* **1990**, *106*, 227.
(72) Blazejowski, J.; Rak, J.; Lampe, F. W. *J. Photochem. Photobiol., A* **1990**, *52*, 347.
(73) Ravi, R.; Takoudis, C. G. *J. Electrochem. Soc.* **1992**, *139*, 1994.

Table 7. Thermodynamic Characteristics of Transition States for Structural Transformations in H_2PPH_2 and $HPPH_3$ Calculated at the 6-31G** Geometries

transition state		thermodynamic quantity[a]						
		$\Delta_{f,298}H^\ominus$			$\Delta_{f,298}G^\ominus$			
structure number[b]	process/molecule (states)	RHF	MP4	QCISD(T)/ 6-311+G(3df,2p)	RHF	MP4	QCISD(T)/ 6-311+G(3df,2p)	$_{298}S^\ominus$
4	rotation/H_2PPH_2 (gauche−gauche)	356.9 (45.3)	186.1 (136.4)	89.5 (63.8)	373.9 (62.3)	203.2 (153.4)	106.5 (80.8)	261.8
5	rotation/H_2PPH_2 (gauche−staggered)	343.2 (31.5)	171.2 (121.5)	75.7 (50.0)	360.3 (48.7)	188.3 (138.6)	92.8 (67.1)	261.5
6	rotation/$HPPH_3$	471.2 (159.5)	295.1 (245.4)	181.3 (155.6)	488.4 (176.8)	312.4 (262.6)	198.6 (172.8)	261.1
7	inversion/H_2PPH_2 (gauche−gauche)	459.4 (147.8)	284.4 (234.7)	182.5 (156.8)	475.7 (164.0)	300.6 (250.9)	198.8 (173.0)	264.5
8	unimolecular tautomerization/H_2PPH_2−$HPPH_3$	670.1 (358.5)	432.7 (383.0)	318.8 (293.1)	686.7 (375.0)	449.3 (399.5)	335.3 (309.6)	263.4

[a] $\Delta_{f,298}H^\ominus$ and $\Delta_{f,298}G^\ominus$ values in kilojoules per mole; $_{298}S^\ominus$ values in joules per mole per kelvin (values in parentheses include isogyric correction). All values correspond to the partition function contributions calculated using all normal frequencies, except the imaginary frequency. [b] For structures, see Figure 4.

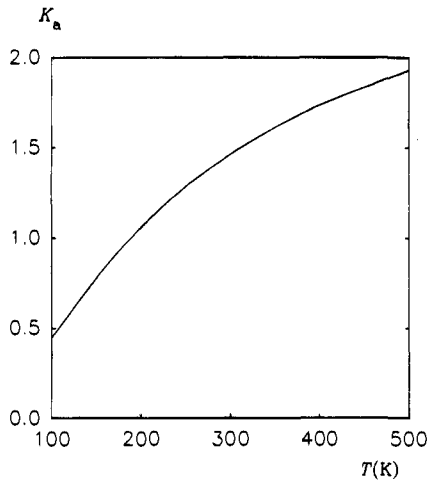

Figure 4. Ratio of the number of staggered to gauche molecules (thermodynamic equilibrium constant K_a for gauche ⇄ staggered transformation) *versus* temperature (T).

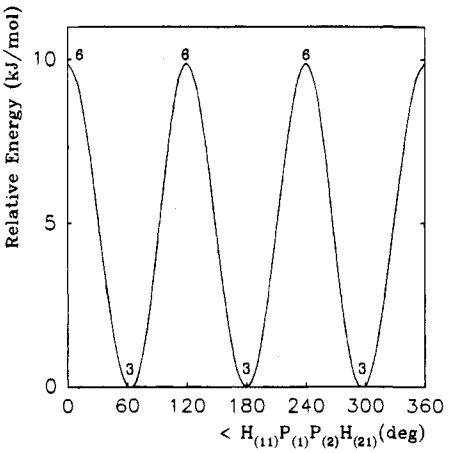

Figure 5. Energy of $HPPH_3$ relative to that of the lowest energy structure (**3** in Figure 1) upon rotation around the P−P bond at the RHF/6-31G** level (numbers indicate structures in Figures 1 and 3).

in Table 9 (Figure 8), the most probable primary process is the P−P bond fission leading to two PH_2 radicals. These radicals are highly reactive and can initiate even chain reactions.[74] Among these processes, hydrogen abstraction from the surrounding molecules leading to PH_3 should be very fast.[74] This explains the formation of large amounts of PH_3 upon the

(74) Blazejowski, J.; Lampe, F. W. *J. Phys. Chem.* **1981**, *85*, 1856.

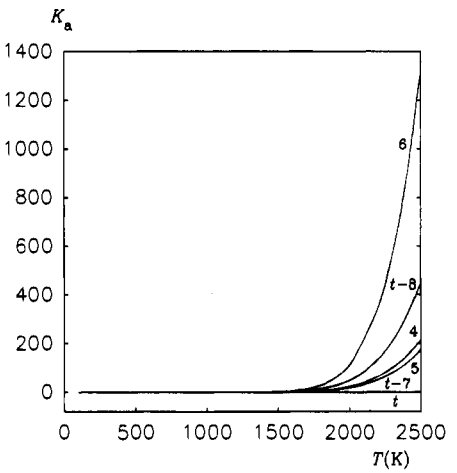

Figure 6. Thermodynamic equilibrium constants (K_a) for tautomerization (t) and decomposition of H_2PPH_2 to singlet (4) or triplet (5) PPH_2, dissociation of H_2PPH_2 toward PH_2 (6), and complex processes like H_2PPH_2 ⇄ $HPPH_3$ ⇄ $^1PH + PH_3$ (*t*-7) or H_2PPH_2 ⇄ $HPPH_3$ ⇄ $^3PH + PH_3$ (*t*-8) *versus* temperature (T) (numeration of reactions is in Table 8). Thermodynamic energy barriers were those relevant to QCISD(T)/6-311+G(3df,2p) (Tables 4 and 8).

decomposition of H_2PPH_2.[2,6,7] PH_3 is much more thermodynamically and kinetically stable than H_2PPH_2 (Tables 8 and 9) and thus remains as a final reaction product. If decomposition of H_2PPH_2 is initiated by H_2 elimination (eq 4), then PPH_2 would immediately decompose toward H_2 and P_2 (eq 9) since the latter process would be much faster than the primary one (Figure 8). This could explain the formation of some phosphorus upon decomposition of diphosphine.[6]

Kinetic considerations describe the behavior of systems that are far from equilibrium. Changes must be such as to attain this state. Therefore, for processes considered above and listed in Table 9 we determined equilibrium constants as functions of temperature. The corresponding plots are shown in Figure 6. The thermodynamic driving force is very weak for the transformation of H_2PPH_2 to $HPPH_3$ (t). As far as decomposition is concerned, diphosphine should be fairly stable up to 1500 K. Just above this temperature, the actual driving forces for dissociation appear. The strongest corresponds to reaction 6, *i.e.*, P−P bond fission. The next strong driving force would be for the dissociation toward PH_3 and triplet PH, with $HPPH_3$ as the intermediate (t-8) (the driving force for a similar process leading to singlet PH is weak, t-8). As in a macroscopic system, the equilibrium between H_2PPH_2 and $HPPH_3$ is reached easily (almost no kinetic barrier over endothermicity); thus, small

Table 8. Kinetic (K) and Thermodynamic (Th) Barriers for Decomposition (d) of Diphosphine and Related Molecules Relevant to 6-31G** Geometries

			quantity[a]									
			$\Delta_d E$			$\Delta_{d,298}H^\ominus$			$\Delta_{d,298}G^\ominus$			
eq no.	reaction[b]	type of barrier	RHF	MP4	QCISD(T)/ 6-311+G(3df,2p)	RHF	MP4	QCISD(T)/ 6-311+G(3df,2p)	RHF	MP4	QCISD(T)/ 6-311+G(3df,2p)	$\Delta_{d,298}S^\ominus$
(4)	$H_2PPH_2 \rightarrow H_2 + {}^1PPH_2$	Th	246.5	208.0	205.3	230.8	192.3	189.6	196.2	157.7	155.0	116.2
		K	283.9	269.5	252.4	272.7	258.3	241.2	271.8	257.4	240.3	3.0
(5)	$H_2PPH_2 \rightarrow H_2 + {}^3PPH_2$	Th	137.4	191.9	209.8	121.4	175.9	193.8	83.9	138.4	156.3	126.0
(6)	$H_2PPH_2 \rightarrow 2^2PH_2$	Th, K	137.6	217.0	239.3	120.0	199.4	221.7	73.8	153.2	175.5	154.9
(7)	$HPPH_3 \rightarrow {}^1PH + PH_3$	Th, K	177.2	221.7	227.5	164.2	208.7	214.5	123.0	167.5	173.3	138.2
(8)	$HPPH_3 \rightarrow {}^3PH + PH_3$	Th	−19.7	66.7	110.4	−32.7	53.7	97.4	−76.6	9.8	53.5	147.3
(9)	${}^1PPH_2 \rightarrow H_2 + P_2$	Th	−53.9	−105.6	−76.0	−64.6	−116.3	−86.7	−91.9	−143.6	−114.0	91.7
		K	229.2	225.7	206.1	216.4	212.9	193.3	216.5	213.0	193.4	−0.3
(10)	${}^3PPH_2 \rightarrow H_2 + P_2$	Th	55.2	−89.4	−80.4	44.8	−99.8	−90.8	20.4	−124.2	−115.2	81.9
(11)	$PH_3 \rightarrow H_2 + {}^1PH$	Th, K	342.7	360.9	346.7	325.0	343.2	329.0	295.8	314.0	299.8	98.1
(12)	$PH_3 \rightarrow H_2 + {}^3PH$	Th	145.9	205.9	229.6	128.1	188.1	211.8	96.2	156.2	179.9	107.2

[a] $\Delta_d E$, $\Delta_{d,298}H^\ominus$ and $\Delta_{d,298}G^\ominus$ values in kilojoules per mole; $\Delta_{d,298}S^\ominus$ values in joules per mole per kelvin. $\Delta_{d,298}H^\ominus$, $\Delta_{d,298}G^\ominus$, and $\Delta_{d,298}S^\ominus$ values for transition states correspond to the partition function contributions calculated using all normal frequencies, except the imaginary frequency. [b] Singlet state of molecules, except where otherwise stated; all species in the lowest energy states.

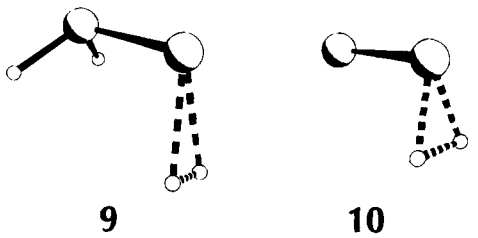

9 **10**

Figure 7. Transition state structures for H_2 elimination from H_2PPH_2 (**9**) and decomposition of PPH_2 to H_2 and P_2 (**10**).

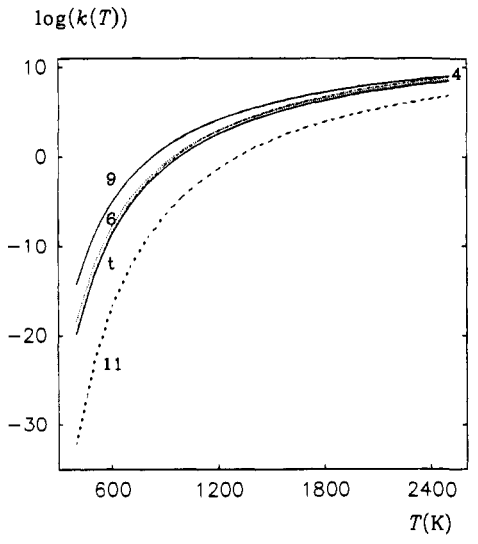

Figure 8. High-pressure-limit rate constants ($k_\infty(T)$ in s^{-1}) for tautomerization (t) and decomposition processes shown in Table 9 *versus* temperature (T). E_0 values used in calculations were kinetic (reactions 4 and 9) or thermodynamic (tautomerization, reactions 6 and 11) energy barriers relevant to QCISD(T)/6-311+G(3df,2p) (Tables 4 and 8). Reaction path degeneracies were assumed to be 4, 2, 1, 1, and 3 for tautomerization and reactions 4, 6, 9, and 11, respectively. Partition functions for substrate and sums of states for activated complex molecules were calculated using theoretically derived frequencies.

amounts of $HPPH_3$ are always present together with H_2PPH_2. If $HPPH_3$ dissapears as the result of reactions 7 or 8 (Table 9), new $HPPH_3$ molecules are instantaneously created. H_2 elimination from H_2PPH_2 accompanied by the formation of both singlet or triplet PPH_2 (eq 4 or 5) would have a moderate driving force, lower than for the two above-mentioned processes.

Both kinetic and thermodynamic considerations enable us to conclude that the most probable primary process upon decomposition of H_2PPH_2 is P−P bond fission. Of secondary importance is H_2 elimination followed by the decomposition of PPH_2 to P_2 and H_2. Thermodynamic considerations do not rule out the possibility of the direct decomposition of H_2PPH_2 to PH_3 and ^3PH, with $HPPH_3$ as the intermediate.

Table 9. Arrhenius Parameters for Unimolecular Processes

process		parameter	
eq no.[a]	scheme	Z	E_a
(*t*)	$H_2PPH_2 \rightleftharpoons HPPH_3$	7.03×10^{13}	258.3
(4)	$H_2PPH_2 \rightarrow H_2 + {}^1PPH_2$	2.08×10^{14}	261.5
(6)	$H_2PPH_2 \rightarrow 2^2PH_2$	5.14×10^{13}	246.3
(9)	${}^1PPH_2 \rightarrow H_2 + P_2$	2.55×10^{13}	212.0
(11)	$PH_3 \rightarrow H_2 + {}^1PH$	1.74×10^{14}	356.1

[a] See Table 8. [b] Z values in s^{-1}; E_a values in kilojoules per mole (both values result from the fit of the equation $k_\infty(T) = Z \exp[-E_a/(RT)]$ to the data predicted by the RRKM theory using a least squares method).

Conclusions

According to the results of theoretical calculations, H_2PPH_2 should exist at ambient temperature in both gauche and staggered forms, although most probably in the latter. Physicochemical properties determined experimentally for diphosphine are consistent with theoretical predictions, *i.e.*, can be interpreted as characteristic for the mixtures of two conformers. These findings do not conform with the results of earlier calculations that, however, did not include the behavior of molecules on a microscopic scale. Previous interpretations of experimental data by other authors seems to concern gauche diphosphine, *i.e.*, only one form of the two existing in the mixture.

A new finding is $HPPH_3$, the tautomeric form of H_2PPH_2. Isolated $HPPH_3$ molecules (*e.g.*, at very low pressure) could exist, owing to the high kinetic barrier to unimolecular tautomerization into H_2PPH_2 or decomposition. However, bimolecular tautomerization, with a negligible kinetic barrier over the thermodynamic energy barrier, maintains equilibrium greatly in favor of H_2PPH_2. Nevertheless, $HPPH_3$ can be considered as an intermediate in chemical processes involving diphosphine.

In this paper, several previously unknown physicochemical and thermochemical characteristics were determined for diphosphine and related species. Particularly important are thermochemical data that could be compared with experimental characteristics on the one side and allowed for insight into the stability of various compounds on the other.

Kinetic and thermodynamic analysis of the reactions involving diphosphine revealed how the ratio of staggered/gauche forms of H_2PPH_2 changes with temperature, what can be said about tautomerization between H_2PPH_2 and $HPPH_3$, and what decomposition processes can occur upon an increase in temperature. This information, obtained for the first time, appeared to be very useful in the analysis of the behavior of diphosphine and related molecules.

The use of *ab initio* methods at the Hartree−Fock level together with the 6-31G** basis set predicts the geometry of phosphorus hydrides with sufficient accuracy. Correct values of energy were, however, obtained just after the inclusion of quadratic configuration interaction with single and double substitutions and triples contribution together with large 6-311+G-(3df,2p) or even 6-311++G(3df,3pd) basis sets. The necessity to carry out such advanced, very time-consuming calculations causes limitations in the application of quantum chemistry methods to phosphorus hydrides. On the other hand, semiempirical MNDO, AM1, and PM3 methods predict both geometry and energetics of the two diphosphine tautomers incorrectly and are thus completely inadequate for this type of molecules.

The compounds examined in this work are those of the simplest derivatives of phosphorus, the element of high importance due to its presence in living matter. Phosphorus compounds also find numerous industrial applications. It is therefore important to know their structure, properties, and behavior, as well as ways of theoretical predictions of these. We believe that this paper sheds new light on the above-mentioned aspects of phosphorus chemistry.

Acknowledgment. The authors thank Dr. M. Gutowski for his valuable comments. The financial support of this work from the Polish State Committee for Scientific Research (KBN) under Grant 2 0679 91 01 (Contract No. 1156/2/91) is gratefully acknowledged.

JA9426960